01 Jan 2007

Photon Angular Distribution and Nuclear-State Alignment in Nuclear Excitation by Electron Capture

Adriana Palffy

Zoltan Harman

Andrey S. Surzhykov

Ulrich D. Jentschura
Missouri University of Science and Technology, ulj@mst.edu

Recommended Citation

A. Palffy et al., "Photon Angular Distribution and Nuclear-State Alignment in Nuclear Excitation by Electron Capture," *Physical Review A - Atomic, Molecular, and Optical Physics*, vol. 75, no. 1, pp. 012712-1-012712-9, American Physical Society (APS), Jan 2007.
The definitive version is available at https://doi.org/10.1103/PhysRevA.75.012712

Photon angular distribution and nuclear-state alignment in nuclear excitation by electron capture

Adriana Pálffy,[1,*] Zoltán Harman,[2] Andrey Surzhykov,[2] and Ulrich D. Jentschura[2]
[1]*Institut für Theoretische Physik, Justus-Liebig-Universität Giessen, Heinrich-Buff-Ring 16, 35392 Giessen, Germany*
[2]*Max-Planck-Institut für Kernphysik, Saupfercheckweg 1, 69117 Heidelberg, Germany*
(Received 30 October 2006; published 17 January 2007)

The alignment of nuclear states resonantly formed in nuclear excitation by electron capture (NEEC) is studied by means of a density matrix technique. The vibrational excitations of the nucleus are described by a collective model and the electrons are treated in a relativistic framework. Formulas for the angular distribution of photons emitted in the nuclear relaxation are derived. We present numerical results for alignment parameters and photon angular distributions for a number of heavy elements in the case of $E2$ nuclear transitions. Our results are intended to help future experimental attempts to discern NEEC from radiative recombination, which is the dominant competing process.

DOI: 10.1103/PhysRevA.75.012712 PACS number(s): 34.80.Lx, 23.20.Nx, 23.20.−g

I. INTRODUCTION

The process studied in this paper consists of two steps. First, a free electron is recombined into an electronic shell of a positive, preferably highly charged ion while resonantly transferring its excess energy to the nucleus. This step is referred to as nuclear excitation by electron capture (NEEC) in the literature. It is the time-reversed process of internal conversion (IC) and can also be regarded as the nuclear analog of dielectronic recombination (DR), where a bound electron is resonantly excited. In the second step, the excited nuclear state thus formed decays radiatively. The whole process is illustrated in Fig. 1. Proposed in Ref. [1], the NEEC recombination mechanism has not been observed experimentally yet.

Related processes at the borderline between nuclear and atomic physics have been experimentally confirmed, such as nuclear excitation by electronic transition (NEET), that is a decay mode of the electron atomic shell in which energy is transferred to the nucleus. NEET has been observed in ^{189}Os [2], ^{237}Np [3], and, most recently, in ^{197}Au [4]. For its time-reversed process, the bound internal conversion (BIC), direct experimental evidence was not found until recently [5].

The detection of the recombined ions or the emitted radiation characteristic for the nuclear decay can be used to observe NEEC experimentally. The position of the peak in the recombination cross section or the spectrum of emitted photons directly yields the nuclear transition energy. The detected spectra may provide further information on nuclear decay mechanisms and level population. Thus the study of NEEC in recombination experiments can also be regarded as a possible tool to investigate nuclear properties.

In a previous paper [6], we presented total NEEC cross sections for a range of heavy isotopes. Recently, the quantum interference of NEEC and the background process of radiative recombination (RR) was investigated [7]. In the present work we study a different aspect, namely, the alignment, i.e., the magnetic sublevel population of the nuclear excited states generated in the resonant recombination process. The alignment of the nuclear excited state also allows one to derive the angular distribution of the radiation emitted in the nuclear relaxation process and the cross section differential with respect to the photon emission angle. Differential cross sections for the similar process of DR have been investigated theoretically [8–11] and experimentally [12,13].

The photon angular distribution is of general interest for experimental implementations aiming at observing NEEC by the detection of radiation. Furthermore, as found in this work, the photon emission pattern is substantially different from the one of the concurrent process of RR, which may help to discern the two channels.

The reorientation of the nuclear axis caused by the electric field of a charged particle that excites the nucleus is a well-studied process in nuclear physics. The change in the nuclear spin directions following the Coulomb excitation of the nucleus by collisions with low-energy charged particles affects the angular distribution of the emitted γ rays [14]. In the case of the electric radiative transitions, NEEC can be regarded as a Coulomb excitation with free electrons that are in the end recombined into a bound state of the ion.

We apply a density matrix formalism to describe the alignment of rotationally excited nuclear states formed by

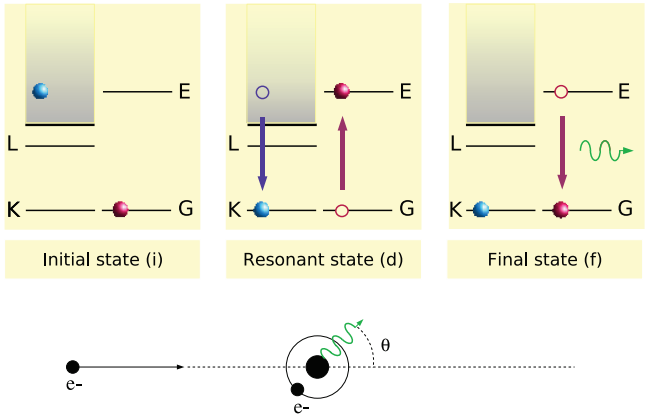

FIG. 1. (Color online) NEEC recombination mechanism of a continuum electron into the K shell of a bare ion. The nucleus is schematically represented as undergoing the transition from the ground state (G) to the excited state (E) and again to its ground state. The bottom figure shows the geometry of the process.

*Electronic address: adriana-claudia.gagyi-palffy@uni-giessen.de

NEEC and the angular distribution of the deexcitation radiation. Nuclear states are treated in the framework of the nuclear collective model and the electrons are described by Dirac four-component wave functions, as necessary for the heavy elements studied here. The electron-nucleus interaction operator is expanded in spherical multipoles to facilitate the evaluation of transition matrix elements. This theoretical approach is presented in detail in Sec. II. NEEC nuclear alignment parameters are presented for the case of $E2$ excitations in heavy highly charged ions and differential cross sections are compared to the same quantity corresponding to the background process of RR in Sec. III. The relevance of these results for future experiments targeting the observation of NEEC is discussed. We briefly summarize the findings of the paper in Sec. IV. Atomic units are used throughout this work unless otherwise specified.

II. THEORETICAL FORMALISM

Since its introduction in 1927 by von Neumann and Landau, the density matrix approach has been found to be a useful and elegant tool in many fields of modern physics. For applications in atomic physics, and combined particularly with the concept of spherical tensors, this approach was originally developed by Fano [15] in the 1950s. Since then, the density matrix theory has been utilized successfully in many case studies on atomic collisions, e.g., for describing the excitation of atomic autoionizing states, polarization effects in radiative and Auger decays, cascade processes, or lifetime interferences in resonantly excited atoms.

In this paper we apply a density matrix formalism to describe the two-step process in which (i) a free (or quasifree) electron is captured into the bound state of an initially bare ion with excitation of the atomic nucleus which (ii) subsequently decays under the emission of characteristic radiation. Because the properties of this radiation are closely related to the alignment of the excited nuclear state, we first have to investigate the population of these states as it arises due to the electron capture process. Therefore, in Sec. II A, we derive the general formulas for the density matrix of the excited nuclear states produced by electron capture. In particular, we show how the sublevel population of these states can be described in terms of the so-called alignment parameters. The calculation of these parameters involves the NEEC transition amplitudes and requires the use of a nuclear model. Following Ref. [6], the NEEC transition amplitudes are derived in Sec. II B. Finally, in Sec. II C we consider the subsequent nuclear decay and obtain the angular distribution of the deexcitation photons with the help of the alignment parameters.

A. Alignment of the excited nuclear state

Within the density matrix theory, the state of a physical system is described in terms of statistical (or density) operators. These operators can be considered to represent, for instance, an ensemble of systems which are—altogether—in either a pure quantum state or in a mixture of different states with any degree of coherence. Then, the basic idea of the density matrix formalism is to accompany such an ensemble through the collision process, starting from a well-defined initial state and by passing through one or, possibly, several intermediate states until the final state of the collision process is attained.

In NEEC, the initial state of the combined system is given by the electron with a well-defined asymptotic momentum $\boldsymbol{p}$ and spin projection m_s, and an ion which is specified in terms of its nuclear charge Z and its initial nuclear spin quantum numbers I_i and projection M_i. (We note here that we consider recombination into bare or closed shell ions, thus the angular momentum of the bound electron shell is zero.) Assuming that these two subsystems, ion and electron, are uncorrelated, the overall initial density operator is given as the direct product of the two initial subsystems' density operators:

$$\rho_i = \rho_{ion} \otimes \rho_e . \tag{1}$$

If neither the electrons nor the ions are polarized initially, an averaging over the magnetic quantum numbers can be performed and the tensor product can be written as

$$\rho_i = \frac{1}{2}\frac{1}{2I_i+1}\sum_{m_s M_i} |\boldsymbol{p} m_s\rangle |N_i I_i M_i\rangle \langle N_i I_i M_i| \langle \boldsymbol{p} m_s|, \tag{2}$$

where N_i denotes all the additional quantum numbers needed for a unique specification of the nuclear states.

In the intermediate state d formed by the capture of the electron, the statistical operators have to describe both the electron in some bound ionic state $|n_d \kappa_d j_d m_d\rangle$ as well as the state of the excited nucleus $|N_d^* I_d M_d\rangle$. Here, n_d, κ_d, j_d, and m_d are the principal quantum number, Dirac angular momentum quantum number, total angular momentum quantum number, and magnetic quantum number of the bound one-electron state, respectively. As known from density matrix theory, the statistical operators of the initial and the (subsequent) intermediate states of the system are connected by

$$\rho_d = T_{en} \rho_i T_{en}^{\dagger}, \tag{3}$$

where T_{en} is the transition operator for the electron-nucleus interaction which causes the nuclear excitation. The particular form of this operator will be given in Sec. II B.

Instead of applying Eq. (3), in practice, it is often more convenient to rewrite the statistical operators in a matrix representation. For instance, in a basis with well-defined angular momenta, the intermediate-state density matrix is given by

$$\begin{aligned} &\langle N_d^* I_d M_d, n_d \kappa_d j_d m_d | \rho_d | N_d^* I_d M_d', n_d \kappa_d j_d m_d' \rangle \\ &\quad = \frac{1}{2}\frac{1}{2I_i+1}\sum_{m_s M_i} \langle N_d^* I_d M_d, n_d \kappa_d j_d m_d | T_{en} | N_i I_i M_i, \boldsymbol{p} m_s \rangle \\ &\qquad \times \langle N_d^* I_d M_d', n_d \kappa_d j_d m_d' | T_{en} | N_i I_i M_i, \boldsymbol{p} m_s \rangle^* , \end{aligned} \tag{4}$$

assuming that both the incident electrons and ions are initially unpolarized [see Eq. (2)]. Indeed, the intermediate-

state density matrix (4) still contains the complete information about the NEEC process and, thus, can be used to derive all the properties of the bound electron and the excited nucleus. For instance, assuming that the magnetic states m_d of the bound electron remain unobserved in the particular experiment, we may characterize the sublevel population of the excited nucleus $|N_d^* I_d\rangle$ in terms of the nuclear density matrix

$$\langle N_d^* I_d M_d|\rho_d^{nucl}|N_d^* I_d M_d'\rangle = \frac{1}{2}\frac{1}{2I_i+1}\sum_{m_s M_i m_d}\langle N_d^* I_d M_d, n_d\kappa_d j_d m_d|T_{en}|N_i I_i M_i, \boldsymbol{p} m_s\rangle \times\langle N_d^* I_d M_d', n_d\kappa_d j_d m_d|T_{en}|N_i I_i M_i, \boldsymbol{p} m_s\rangle^*, \quad (5)$$

which is obtained from Eq. (4) by taking the trace over all unobserved quantum numbers of the electron.

As seen from Eq. (5), the information about the states of the excited nucleus produced by the electron capture into the ion is now contained in the transition matrix elements $\langle N_d^* I_d M_d, n_d\kappa_d j_d m_d|T_{en}|N_i I_i M_i, \boldsymbol{p} m_s\rangle$. These matrix elements contain the wave function $|\boldsymbol{p} m_s\rangle$ of a free electron with a definite asymptotic momentum. For further simplification of the intermediate nuclear spin-density matrix, it is therefore necessary to decompose this continuum wave into partial waves $|\epsilon\kappa j m\rangle$, in order to apply later the standard techniques from the theory of angular momentum. As discussed previously [16], however, special care has to be taken about the choice of the quantization axis since this directly influences the particular form of the partial wave decomposition. Using, for example, the direction of the electron momentum $\boldsymbol{p}$ as the quantization axis, the full expansion of the continuum wave function is given by [16]

$$|\boldsymbol{p} m_s\rangle = \sum_\kappa i^l e^{i\Delta_\kappa}\sqrt{4\pi(2l+1)}\langle l 01/2 m_s|j m_s\rangle|\epsilon\kappa j m_s\rangle, \quad (6)$$

where the summation runs over all partial waves $\kappa = \pm 1, \pm 2, \ldots$, along all values of Dirac's angular momentum quantum number $\kappa = \pm(j+1/2)$ for $l = j \pm 1/2$. The symbol $\langle j_1 m_1\ j_2 m_2|j_{12} m_{12}\rangle$ generally represents the Clebsch-Gordan coefficients for the coupling of two angular momenta j_1 and j_2 to j_{12}. In our notation, the orbital momentum l represents the parity $(-1)^l$ of the partial waves $|\epsilon\kappa j m_s\rangle$, and Δ_κ is the Coulomb phase shift given by [16]

$$\Delta_\kappa = \frac{1}{2}\arg\left(\frac{-\kappa + i\nu/W}{s + i\nu}\right) - \arg(\Gamma(s + i\nu)) + \frac{\pi(l+1-s)}{2}, \quad (7)$$

with $W = E\alpha^2$, $\nu = \alpha Z W/\sqrt{W^2-1}$, and $s = \sqrt{\kappa^2 - (\alpha Z)^2}$. Here, α is the fine-structure constant and E is the total electron energy. In the case of capture into ions with an initially closed shell—i.e., He-like—configuration, the phases can be approximated by using an effective nuclear charge of $Z_{\text{eff}} = Z - N_b$ in Eq. (7), with N_b being the number of bound electrons in the ion. The sufficiency of this approximation is confirmed by calculating the electrostatic potential induced by the screening electrons in the Dirac-Fock approximation [17] and numerically determining the phases for the combined nuclear and screening potentials.

Using the decomposition (6) of the continuum wave function, the intermediate nuclear density matrix (5) can be rewritten in the form

$$\langle N_d^* I_d M_d|\rho_d^{nucl}|N_d^* I_d M_d'\rangle = \frac{1}{2}\frac{4\pi}{2I_i+1}\sum_{m_s M_i m_d}\sum_{\kappa\kappa'} i^{l-l'} e^{i(\Delta_\kappa - \Delta_{\kappa'})}\sqrt{(2l+1)(2l'+1)} \times\langle l 01/2 m_s|j m_s\rangle\langle N_d^* I_d M_d, n_d\kappa_d j_d m_d|T_{en}|N_i I_i M_i, \epsilon\kappa j m_s\rangle \times\langle l' 01/2 m_s|j' m_s\rangle \times\langle N_d^* I_d M_d', n_d\kappa_d j_d m_d|T_{en}|N_i I_i M_i, \epsilon\kappa' j' m_s\rangle^*. \quad (8)$$

Equation (8) represents the most general form of the intermediate nuclear density matrix which can now be used to study the properties of the excited nucleus $|N_d^* I_d\rangle$ following the capture of a free electron. For the analysis of the radiative deexcitation of such a nucleus, however, it is more convenient to represent its intermediate state in terms of the statistical tensors of rank k

$$\rho_{kq}(N_d^* I_d) = \sum_{M_d M_d'}(-1)^{I_d - M_d'}\langle I_d M_d I_d - M_d'|kq\rangle \times\langle N_d^* I_d M_d|\rho_d^{nucl}|N_d^* I_d M_d'\rangle. \quad (9)$$

Although both the density matrix (8) and the statistical tensors (9) contain the same physical information, the latter form enables one to exploit the rotational symmetry of free atoms and ions. By inserting the density matrix (8) into the definition (9), we finally obtain the statistical tensors of the intermediate state as

$$\rho_{kq}(N_d^* I_d) = \frac{4\pi}{2(2I_i+1)}\sum_{m_s M_i m_d}\sum_{\kappa\kappa'}\sum_{M_d M_d'} i^{l-l'} e^{i(\Delta_\kappa - \Delta_{\kappa'})} \times\sqrt{(2l+1)(2l'+1)}(-1)^{I_d - M_d'} \times\langle l 01/2 m_s|j m_s\rangle\langle l' 01/2 m_s|j' m_s\rangle\langle I_d M_d I_d - M_d'|kq\rangle \times\langle N_d^* I_d M_d, n_d\kappa_d j_d m_d|T_{en}|N_i I_i M_i, \epsilon\kappa j m_s\rangle \times\langle N_d^* I_d M_d', n_d\kappa_d j_d m_d|T_{en}|N_i I_i M_i, \epsilon\kappa' j' m_s\rangle^*. \quad (10)$$

Further evaluation of these statistical tensors within the framework of the nuclear collective model is discussed in the next section. The spin state of the excited nucleus is described by the reduced statistical tensors or alignment parameters

$$\mathcal{A}_k(N_d^* I_d) = \frac{\rho_{k0}(N_d^* I_d)}{\rho_{00}(N_d^* I_d)}, \quad (11)$$

which are directly related to the cross section for the population of the different nuclear magnetic sublevels $|N_d^* I_d M_d\rangle$.

B. Calculation of the transition amplitudes

The expression of the statistical tensors involves the matrix element of the transition operator T_{en} that describes the electron-nucleus interaction in the case of electric transitions of the nucleus. We adopt in the following the Coulomb gauge as it allows the separation of the dominant Coulomb interaction between the electronic and nuclear degrees of freedom. The transition operator corresponds in lowest order to the interaction Hamiltonian H_{en} applied in [6]:

$$T_{en} = \int d^3 r_n \frac{\rho_n(\vec{r}_n)}{|\vec{r}_e - \vec{r}_n|}. \tag{12}$$

In the above equation, $\rho_n(\vec{r}_n)$ is the nuclear charge density, $\vec{r}_n$ denotes the nuclear coordinate, and $\vec{r}_e$ the electronic coordinate. The integration is performed over the whole nuclear volume. The matrix element of the transition operator T_{en} enters the expression of the NEEC rate for electric transitions [6]

$$Y_n^{i\to d} = \frac{2\pi}{2(2I_i+1)} \sum_{M_i m_s} \sum_{M_d m_d} \times \int d\Omega_p |\langle N_d^* I_d M_d, n_d \kappa_d j_d m_d | T_{en} | N_i I_i M_i, \boldsymbol{p} m_s \rangle|^2 \rho_i, \tag{13}$$

where ρ_i is the density of the initial electronic states and $\int \Omega_p$ denotes integration over all possible directions of the incoming electron.

In order to describe the nuclear transition we use a phenomenological collective model [18] that interprets the characteristic band structures in the energy range up to 2 MeV in the case of deformed even-even nuclei as vibrations and rotations of the nuclear surface. The even-even nuclei have usually a low-lying 2^+ first excited state, which is characterized by a strong electric $E2$ transition to the ground state. The nuclear surface is parametrized as

$$R(\theta_n, \varphi_n) = R_0 \left(1 + \sum_{\ell=0}^{\infty} \sum_{m=-\ell}^{\ell} \alpha_{\ell m}^* Y_{\ell m}(\theta_n, \varphi_n) \right), \tag{14}$$

where the amplitudes $\alpha_{\ell m}$ describe the deviations of the nuclear surface with respect to the sphere of radius R_0 and thus serve as collective coordinates. Using this parametrization and requiring that the charge be homogeneously distributed, the nuclear charge density can be written as

$$\rho_n(\vec{r}_n) = \rho_0 \Theta(R(\theta_n, \varphi_n) - r_n), \tag{15}$$

with the constant charge density of the undeformed nucleus given by $\rho_0 = \frac{3Z}{4\pi R_0^3}$. Performing a Taylor expansion of the Heaviside function $\Theta(R - r_n)$ around R_0 we obtain

$$\rho_n(\vec{r}_n) = \rho_0 \Theta(R_0 - r_n) + \rho_0 \delta(r_n - R_0) R_0 \sum_{\ell m} \alpha_{\ell m}^* Y_{\ell m}(\theta_n, \varphi_n) + \cdots. \tag{16}$$

As the vibration amplitudes of the nuclear surface are supposed to be small, we neglect the terms of higher order in the collective coordinates $\alpha_{\ell m}$. While the first term $\rho_0 \Theta(R_0 - r_n)$ in the above equation corresponds to a round nucleus in its ground state, the second term is characterizing the nuclear excitation and enters the expression of the transition operator T_{en} in Eq. (12) [6]. We can therefore write the transition operator as

$$T_{en} = \rho_0 R_0 \sum_{\ell m} \alpha_{\ell m}^* \int d^3 r_n \frac{\delta(r_n - R_0) Y_{\ell m}(\theta_n, \varphi_n)}{|\vec{r}_e - \vec{r}_n|}. \tag{17}$$

It is more convenient to express the collective coordinates $\alpha_{\ell m}$ in terms of the spherical components of the electric multipole transition moment $Q_{\ell m}$, defined as [19]

$$Q_{\ell m} = \int d^3 r r^\ell Y_{\ell m}(\theta, \varphi) \rho_n(\vec{r}). \tag{18}$$

The interaction that accounts for the electric transitions of the nucleus then yields

$$T_{en} = \sum_{\ell m} \frac{Q_{\ell m}}{R_0^\ell} \int d^3 r_n \frac{\delta(r_n - R_0) Y_{\ell m}^*(\theta_n, \varphi_n)}{|\vec{r}_e - \vec{r}_n|}. \tag{19}$$

In the calculation of the matrix element, we use the multipole expansion

$$\frac{1}{|\vec{r}_e - \vec{r}_n|} = \sum_{L=0}^{\infty} \sum_{M=-L}^{L} \frac{4\pi}{2L+1} Y_{LM}(\theta_n, \varphi_n) Y_{LM}^*(\theta_e, \varphi_e) \frac{r_<^L}{r_>^{L+1}}, \tag{20}$$

where $r_<$ and $r_>$ stand for the smaller and the larger of the two radii r_e and r_n, respectively. The integration over the nuclear angular coordinates brings us to the following expression for the Coulomb interaction:

$$T_{en} = \sum_{LM} \frac{4\pi}{2L+1} \frac{Q_{LM}}{R_0^L} Y_{LM}^*(\theta_e, \varphi_e) \int_0^\infty dr_n r_n^2 \frac{r_<^L}{r_>^{L+1}} \delta(r_n - R_0). \tag{21}$$

The matrix element of the transition operator reads

$$\langle N_d^* I_d M_d, n_d \kappa_d j_d m_d | T_{en} | N_i I_i M_i, \epsilon \kappa j m_s \rangle = \frac{1}{R_0^L} \sum_{LM} \frac{4\pi}{2L+1} \langle N_d^* I_d M_d | Q_{LM} | N_i I_i M_i \rangle \times \left\langle n_d \kappa_d j_d m_d \left| Y_{LM}^*(\theta_e, \varphi_e) \int_0^\infty dr_n r_n^2 \frac{r_<^L}{r_>^{L+1}} \delta(r_n - R_0) \right| \epsilon \kappa j m_s \right\rangle. \tag{22}$$

We write the matrix element of the electron-nucleus interaction operator as a product of the nuclear and electronic parts. It is more convenient to use the reduced matrix element of the electric multipole operator Q_{LM}, defined as [20]

$$\langle N_d^* I_d M_d | Q_{LM} | N_i I_i M_i \rangle = \frac{(-1)^{I_i - M_i}}{\sqrt{2L+1}} \langle I_d M_d I_i - M_i | LM \rangle \langle N_d^* I_d \| Q_L \| N_i I_i \rangle. \quad (23)$$

The modulus square of the reduced matrix element of the electric multipole operator can be related to the reduced electric (E) transition probability of a certain multipolarity L,

$$B(EL, I_i \to I_d) = \frac{1}{2I_i + 1} |\langle N_d^* I_d \| Q_L \| N_i I_i \rangle|^2, \quad (24)$$

whose value can be taken from experimental results. For a given multipolarity L, the matrix element can be written as

$$\langle N_d^* I_d M_d, n_d \kappa_d j_d m_d | T_{en} | N_i I_i M_i, \epsilon \kappa j m_s \rangle = \sum_{\mu=-L}^{L} (-1)^{I_d + M_i + L + \mu + m_s + 3j_d} R_0^{-(L+2)} R_{L,\kappa_d,\kappa} \langle N_d^* I_d \| Q_L \| N_i I_i \rangle \times \sqrt{2j_d + 1} \sqrt{\frac{4\pi}{(2L+1)^3}} \langle I_i - M_i I_d M_d | L\mu \rangle \times \langle j - m_s j_d m_d | L - \mu \rangle \langle j_d 1/2 L 0 | j 1/2 \rangle, \quad (25)$$

with the electronic radial integral $R_{L,\kappa_d,\kappa}$ given by

$$R_{L,\kappa_d,\kappa} = \frac{1}{R_0^{L-1}} \int_0^{R_0} dr_e r_e^{L+2} [f_{n_d\kappa_d}(r_e) f_{\epsilon\kappa}(r_e) + g_{n_d\kappa_d}(r_e) g_{\epsilon\kappa}(r_e)] + R_0^{L+2} \int_{R_0}^{\infty} dr_e r_e^{-L+1} [f_{n_d\kappa_d}(r_e) f_{\epsilon\kappa}(r_e) + g_{n_d\kappa_d}(r_e) g_{\epsilon\kappa}(r_e)]. \quad (26)$$

In the electronic radial integrals, $g_{\epsilon\kappa}$ and $f_{\epsilon\kappa}$ are the large and small radial components of the relativistic partial continuum electron wave function

$$\phi_{\epsilon\kappa j m_s}(\vec{r}_e) = \langle \vec{r}_e | \epsilon\kappa j m_s \rangle = \begin{pmatrix} g_{\epsilon\kappa}(r_e) \Omega_\kappa^{m_s}(\theta_e, \varphi_e) \\ i f_{\epsilon\kappa}(r_e) \Omega_{-\kappa}^{m_s}(\theta_e, \varphi_e) \end{pmatrix}, \quad (27)$$

and $g_{n_d\kappa_d}$ and $f_{n_d\kappa_d}$ are the components of the bound Dirac wave functions

$$\phi_{n_d\kappa_d j_d m_d}(\vec{r}_e) = \langle \vec{r}_e | n_d \kappa_d j_d m_d \rangle = \begin{pmatrix} g_{n_d\kappa_d}(r_e) \Omega_{\kappa_d}^{m_d}(\theta_e, \varphi_e) \\ i f_{n_d\kappa_d}(r_e) \Omega_{-\kappa_d}^{m_d}(\theta_e, \varphi_e) \end{pmatrix}, \quad (28)$$

with the spherical spinor functions Ω_κ^m. The radial integral $R_{L,\kappa_d,\kappa}$ is calculated numerically. For the particular case of the $0^+ \to 2^+$ $E2$ transitions, the transition amplitude reads

$$\langle N_d^* 2 M_d, n_d \kappa_d j_d m_d | T_{en} | N_i 00, \epsilon\kappa j m_s \rangle = \frac{\sqrt{4\pi}}{\sqrt{125}} R_0^{-4} (-1)^{M_d + m_s + 3j_d} \sqrt{2j_d + 1} \times \langle N_d^* 2 \| Q_2 \| N_i 0 \rangle \times \langle j - m_s j_d m_d | 2 - M_d \rangle \langle j_d 1/2\ 20 | j 1/2 \rangle R_{2,\kappa_d,\kappa}. \quad (29)$$

The Clebsch-Gordan coefficient $\langle j - m_s\ j_d m_d | 2 - M_d \rangle$ imposes that $M_d = m_s - m_d$, therefore $M_d = M_d'$ and $q = 0$ in Eq. (10).

C. Radiative deexcitation of the nucleus

By making use of the multipole transition amplitudes (25), we are able to calculate now the alignment parameters (11) of the nucleus excited by electron capture. A detailed knowledge of the alignment parameters is required for the analysis of the subsequent deexcitation of the nucleus which may result in the emission of one (or several) photons until the nuclear ground state is reached. This photon emission is characterized (apart from its known energy) by its angular distribution and polarization. The relations of both of these properties to the alignment $\mathcal{A}_k$ of the excited nuclear state are well-known since the early 1960s and have been discussed in detail elsewhere [21–24]. In the present work, therefore, we will restrict ourselves to a rather short account of the basic formulas. For instance, the angular distribution of the gamma rays emitted in the transition from the excited state $|N_d^* I_d M_d\rangle$ to the nuclear ground state $|N_f I_f M_f\rangle$ is given by

$$\frac{d\sigma_{\mathrm{NEEC}}}{d\Omega}(\theta) = \frac{\sigma_{\mathrm{NEEC}}}{4\pi} \left(1 + \sum_{k=2,4,\ldots} f_k(N_d^* I_d, N_f I_f) \mathcal{A}_k(N_d^* I_d) P_k(\cos\theta) \right), \quad (30)$$

where σ_{NEEC} is the total cross section for NEEC followed by the radiative decay of the excited nucleus and θ denotes the angle of the photons with respect to the momentum $\boldsymbol{p}$ of the incoming electrons (chosen as the z-axis). As seen from Eq. (30), the angular dependence of the photon emission results from the Legendre polynomials $P_k(\cos\theta)$ which are weighted by the alignment parameters $\mathcal{A}_k(N_d^* I_d)$ and the coefficients $f_k(N_d^* I_d, N_f I_f)$. In contrast to the alignment parameters, these geometrical coefficients are independent on the nuclear excitation process and just account for the initial and the final nuclear states [23–25],

$$f_k(N_d^* I_d, N_f I_f) = \frac{\sqrt{2I_d+1}}{2} \sum_{LL'pp'} i^{L'+p'-L-p}(-1)^{I_f+I_d+k+1}\sqrt{(2L+1)(2L'+1)}\langle L1L'-1|k0\rangle$$
$$\times[1+(-1)^{L+p+L'+p'-k}]\begin{Bmatrix} L & L' & k \\ I_d & I_d & I_f \end{Bmatrix} \frac{\langle N_d^* I_d \| T_{nr}(L,p) \| N_f I_f\rangle^* \langle N_d^* I_d \| T_{nr}(L',p') \| N_f I_f\rangle}{\sum_{Lp} |\langle N_d^* I_d \| T_{nr}(L,p) \| N_f I_f\rangle|^2}. \quad (31)$$

Here, $\langle N_d^* I_d \| T_{nr}(L,p) \| N_f I_f\rangle$ denotes the reduced matrix element for the $|N_d^* I_d M_d\rangle \rightarrow |N_f I_f M_f\rangle$ decay under the emission of a photon with angular momentum (or multiplicity) L and parity $(-1)^{p+L}$. The form of the nucleus-radiation field multipole interaction operator $T_{nr}(L,p)$ is given in, e.g., Refs. [7,19].

Equations (30) and (31) display the general form of the photon angular distribution for the decay of an aligned system [23,25]. This angular distribution includes all multipoles of the photon field which are allowed for the given radiative transition. In the particular case of the $2^+ \rightarrow 0^+$ nuclear decay, only the electric quadrupole transition $E2$ is allowed by the selection rules for which Eq. (30) simplifies to

$$\frac{d\sigma_{\mathrm{NEEC}}}{d\Omega}(\theta) = \frac{\sigma_{\mathrm{NEEC}}}{4\pi} W(\theta), \quad (32)$$

with the angular distribution given by

$$W(\theta) = \left(1 - \frac{\sqrt{70}}{14}\mathcal{A}_2 P_2(\cos\theta) - \frac{2\sqrt{14}}{7}\mathcal{A}_4 P_4(\cos\theta)\right). \quad (33)$$

As seen from the expression above, the angular distribution of the electric quadrupole transition is entirely determined by the alignment parameters $\mathcal{A}_2$ and $\mathcal{A}_4$ of the excited 2^+ nuclear state and the geometrical coefficients. In the next section we calculate these parameters and, hence, the angular distribution of the deexcitation photons for the electron capture into the $1s_{1/2}$ and $2s_{1/2}$ states of initially bare or He-like $^{174}_{70}$Yb, $^{170}_{68}$Er, $^{154}_{64}$Gd, and $^{162}_{66}$Dy ions.

III. RESULTS AND DISCUSSION

In this section we present the alignment parameters and the angular distribution of the emitted photons that follow NEEC into the $1s$ orbitals of bare ions and the $2s$ states of initially He-like ions. We consider the even-even nuclei $^{174}_{70}$Yb, $^{170}_{68}$Er, $^{154}_{64}$Gd, and $^{162}_{66}$Dy for which NEEC total cross sections for the capture into the K-shell have been presented in Ref. [6]. The reduced transition probability $B(E2, 0 \rightarrow 2)$ for these nuclei as well as the energies of the nuclear transitions are taken from Ref. [26]. The calculation of the statistical tensors involves the numerical integration of $R_{L,\kappa_d,\kappa}$. For the continuum electron we use relativistic Coulomb-Dirac wave functions, applying the approximation that the nucleus is a pointlike charge. We assume that the free electron, which is far away from the ion, is not sensitive to the internal structure or size of the nucleus. The radial wave functions have been calculated using the same computer routine as in Ref. [6] and cross-checked with the program described in Ref. [27]. The Coulomb phases calculated according to Eq. (7) do not include the effect of the finite nuclear size, which is expected to be negligible. For the continuum electrons recombining into the $2s$ orbital of an initially He-like ion, we

TABLE I. Partial wave phase shifts (Δ_κ, in radians) for capture into the $1s$ and $2s$ orbital of bare ions (Coulomb phases, third and fourth columns) and into the $1s^2 2s$ state of initially He-like ions, in different approximations. In the fifth column, phases for He-like ions with an effective nuclear charge $Z_{\mathrm{eff}}=Z-2$ are given and the last column (DF) contains phases corrected for bound electron screening in the Dirac-Fock approximation.

			$2s$		
$^A_Z X$	κ	$1s$ $\Delta_\kappa(Z_{\mathrm{eff}}=Z)$	$\Delta_\kappa(Z_{\mathrm{eff}}=Z)$	$\Delta_\kappa(Z_{\mathrm{eff}}=Z-2)$	Δ_κ(DF)
$^{154}_{64}$Gd	2	2.313	2.507	2.524	2.529
	−3	−0.913	−0.731	−0.709	−0.706
$^{162}_{66}$Dy	2	0.747	2.246	2.270	2.273
	−3	−2.461	−0.983	−0.954	−0.952
$^{170}_{68}$Er	2	0.805	2.254	2.277	2.280
	−3	−2.408	−0.980	−0.952	−0.951
$^{174}_{70}$Yb	2	5.293	2.205	2.229	2.231
	−3	2.079	−1.033	−1.004	−1.003

TABLE II. Alignment parameters for the 2^+ excited nuclear state formed by NEEC. We denote the capture orbital by nl_j and E_c is the energy of the continuum electron at the resonance.

${}^{A}_{Z}X$	E_c(keV)	nl_j	$\mathcal{A}_2$	$\mathcal{A}_4$
${}^{154}_{64}$Gd	64.005	$1s_{1/2}$	−1.183	1.547
${}^{164}_{66}$Dy	10.318	$1s_{1/2}$	−1.185	1.557
${}^{170}_{68}$Er	11.350	$1s_{1/2}$	−1.183	1.548
${}^{174}_{70}$Yb	4.897	$1s_{1/2}$	−1.181	1.542
${}^{154}_{64}$Gd	108.847	$2s_{1/2}$	−1.146	1.383
${}^{164}_{66}$Dy	58.164	$2s_{1/2}$	−1.090	1.135
${}^{170}_{68}$Er	62.317	$2s_{1/2}$	−1.073	1.056
${}^{174}_{70}$Yb	59.106	$2s_{1/2}$	−1.029	0.861

use an effective nuclear charge number of $Z_{\text{eff}}=Z-2$. This approximation is assumed to be sufficient for the present level of accuracy. We consider relativistic wave functions calculated with the GRASP92 package [28] for the bound state. The finite size of the nucleus, i.e., its nonzero radius R_0, is considered in the bound wave functions and has a sensitive effect on the innershell level energies of the bound electron. The nuclear radius in calculated according to the semiempirical formula [29]

$$R_0 = (1.0793A^{1/3} + 0.73587)\ \text{fm}, \tag{34}$$

where A is the atomic mass number.

In the case of recombination into the $2s$ orbital of an initially He-like ion, the phase shifts of the partial continuum wave functions were calculated by considering the Dirac-Fock (DF) approximation of the $1s^2$ ground state seen by the free electron. As shown in Table I, the difference between such a calculation and the $Z_{\text{eff}}=Z-2$ full screening approximation is very small in the Coulomb phase, less than 0.01 rad, and has a negligible effect on the alignment parameters. In Table I we present the Coulomb phases for the capture into the $1s$ orbital and $2s$ orbitals of the considered ions, the latter calculated using both approximations.

The values of the alignment parameters $\mathcal{A}_2$ and $\mathcal{A}_4$ of the 2^+ excited nuclear states are presented in Table II. Capture into the $1s$ as well as the $2s$ orbitals are considered. The alignment of the excited nuclear state characterized by these parameters gives in the second step of NEEC the angular distribution of the emitted radiation. In Fig. 2 we present the angular distribution $W(\theta)$ given in Eq. (33) for the capture into the $1s$ and $2s$ shells of ${}^{154}_{64}$Gd, ${}^{162}_{66}$Dy, ${}^{170}_{68}$Er, and ${}^{174}_{70}$Yb, respectively. The angular patterns are similar for all four ions, as they all involve $E2$ transitions of nuclei with near

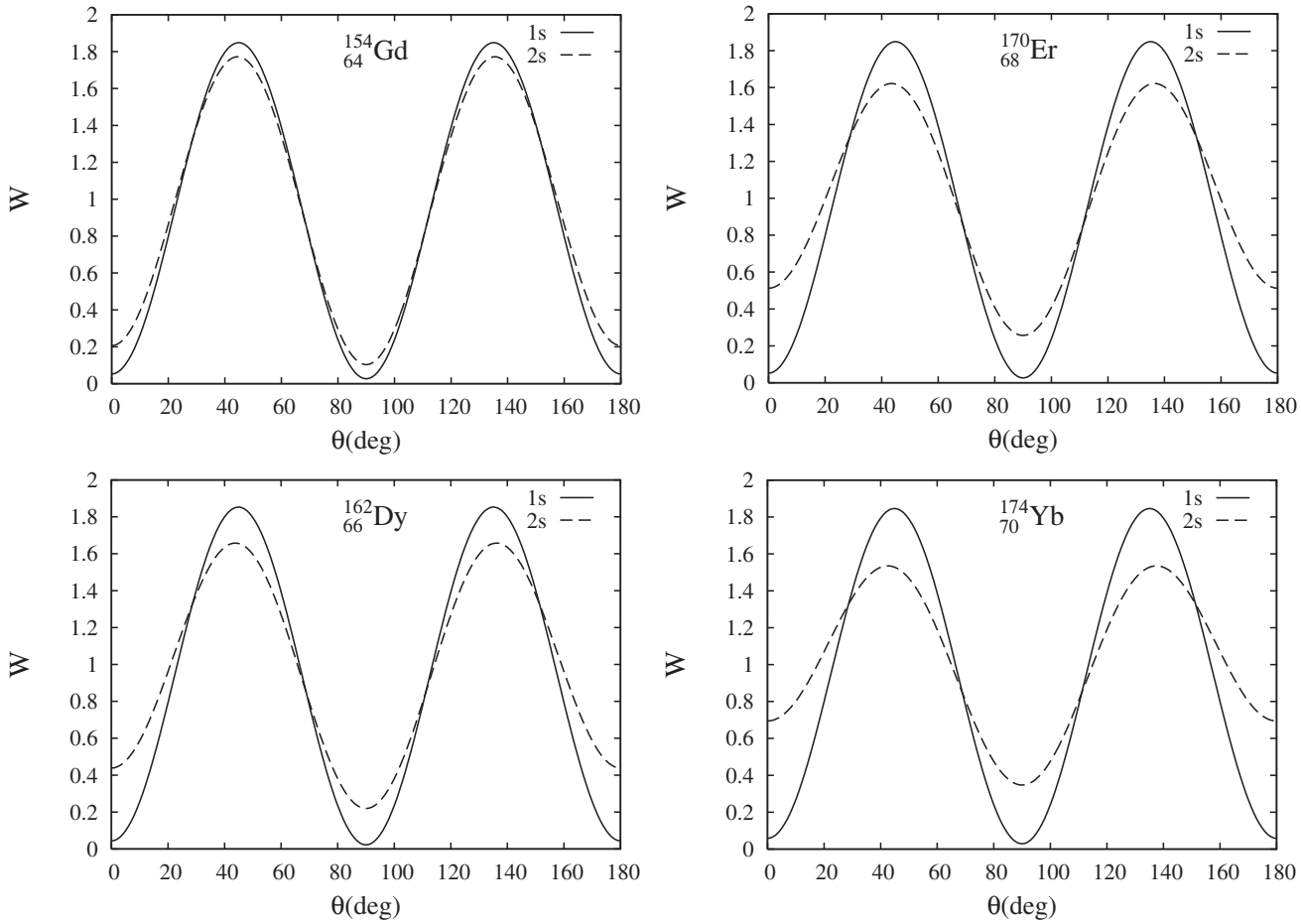

FIG. 2. Angular distribution $W(\theta)$ of photons emitted in the radiative nuclear decay of the 2^+ excited state following NEEC for the elements ${}^{154}_{64}$Gd, ${}^{164}_{66}$Dy, ${}^{170}_{68}$Er, and ${}^{174}_{70}$Yb, respectively. The cases of recombination into the $1s$ state of initially bare ions (solid lines) and into the $2s$ orbital of initially He-like ions (dashed lines) are presented.

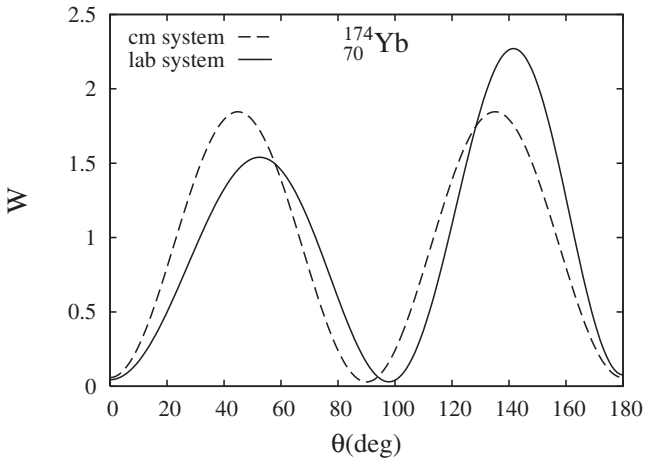

FIG. 3. Angular distribution of the photons with respect to the laboratory (lab) and center-of-mass (cm) systems for the case of NEEC into the 1*s* orbital of Yb^{70+}.

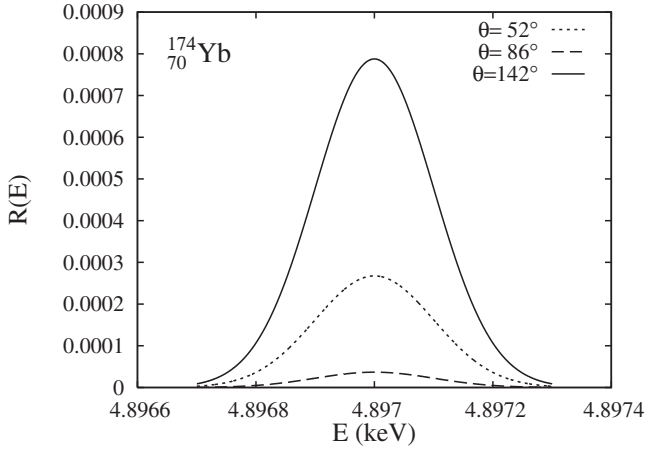

FIG. 4. The NEEC and RR angular differential cross section ratio for the case of $^{174}_{70}$Yb as a function of the continuum electron energy for three different photon emission angles. The NEEC total cross section was convoluted with a Gaussian electron energy distribution with the width parameter of 0.1 eV for a better visual representation of the data.

atomic and mass numbers. Both radiations following the capture into the 1*s* and 2*s* orbitals of the ion present maxima at $\theta=45°$ and $\theta=135°$, a pattern which significantly differs from that of RR [30]. While for the capture into the 1*s* orbitals the radiation intensity emitted at $\theta=0°$, 90°, and 180° appears to be negligible, the pattern for the capture into 2*s* displays larger minimum values at these angles. In contrast to NEEC, the radiative recombination of the free electron is dominated by the *E*1 transition and has an angular distribution (roughly given by a $\sin^2\theta$ function) with a maximum at $\theta=78°$ in the center-of-mass frame.

As the RR and NEEC angular distributions of the emitted photons have maxima at different values of θ, we calculate the ratio between the two angular differential cross sections at different emission angles,

$$R(E) = \left(\frac{d\sigma_{\mathrm{NEEC}}}{d\Omega}(E,\theta) \Big/ \frac{d\sigma_{\mathrm{RR}}}{d\Omega}(E,\theta) \right)\Bigg|_{\theta=\theta_{\max}}, \quad (35)$$

for the case of electron capture into bare ytterbium. We consider here the angles $\theta_{\max}=45°$, 78°, and 135° that correspond to the maxima of NEEC and RR radiation angular distributions. The NEEC total cross section is convoluted with the energy distribution of the continuum electrons assuming a Gaussian width parameter of 0.1 eV. The RR angular differential cross section is calculated within the framework of Dirac's relativistic equation and by taking into account the higher (nondipole) terms in the expansion of the electron-photon interaction [16,30,31]. We assume that the RR and NEEC alignment parameters are constant on the studied energy interval of approximately 1 eV.

We envisage the scenario of a possible NEEC experiment in a storage ring, in which the radiation is emitted by the nucleus of the Yb^{69+} ion moving relativistically with respect to the laboratory frame. A Lorentz transformation of the NEEC and RR angular differential cross sections in the center-of-mass frame is therefore required in order to obtain the quantities in the laboratory system. The angular differential cross section in the laboratory system can be written as [16]

$$\frac{d\sigma(\theta)}{d\Omega} = \frac{1}{\gamma^2(1-\beta\cos\theta)^2}\frac{d\sigma'(\theta')}{d\Omega'}, \quad (36)$$

where $d\sigma'(\theta')/d\Omega'$ is the differential cross section in the center-of-mass system, denoted until now by the unprimed symbols. In our case the reduced velocity β is 0.138 and the Lorentz factor is $\gamma=1.009$. The angle of the photons in the laboratory frame θ is related to the one in the ion-fixed frame θ' by

$$\cos\theta' = \frac{\cos\theta-\beta}{1-\beta\cos\theta}. \quad (37)$$

As the system possesses azimuthal symmetry, $\varphi'=\varphi$. The angular distribution of the photons with respect to the laboratory system for the case of ytterbium is presented in Fig. 3.

In Fig. 4 we present the ratio in Eq. (35) as a function of the continuum electron energy for the three values of the photon emission angle θ in the laboratory frame for which $d\sigma_{\mathrm{NEEC}}(\theta)/d\Omega$ or $d\sigma_{\mathrm{RR}}(\theta)/d\Omega$ have a maximum. In the laboratory frame, the NEEC angular distribution has maxima at $\theta=52°$ and 142°, while in the case of RR the peak is at approximately $\theta=86°$. The ratio of the NEEC and RR angular differential cross sections is more than one order of magnitude larger for $\theta=52°$ and 142° than in the case of $\theta=86°$. If the photons emitted perpendicular to the direction of the incoming electron are measured in an experiment, it is most likely that only the RR background will be detected, as the NEEC differential cross section presents a minimum at $\theta=98°$. For the emission angles $\theta=52°$ and 142° the RR contribution at the resonance electron energy E_c is considerably lower in comparison to the total cross sections of the recombination process,

$$\left(\frac{d\sigma_{\mathrm{NEEC}}}{d\Omega}(E_c,\theta)\Big/\frac{d\sigma_{\mathrm{RR}}}{d\Omega}(E_c,\theta)\right)\Bigg|_{\theta=52^\circ}\simeq 1.5\frac{\sigma_{\mathrm{NEEC}}(E_c)}{\sigma_{\mathrm{RR}}(E_c)}, \tag{38}$$

$$\left(\frac{d\sigma_{\mathrm{NEEC}}}{d\Omega}(E_c,\theta)\Big/\frac{d\sigma_{\mathrm{RR}}}{d\Omega}(E_c,\theta)\right)\Bigg|_{\theta=142^\circ}\simeq 4.4\frac{\sigma_{\mathrm{NEEC}}(E_c)}{\sigma_{\mathrm{RR}}(E_c)}. \tag{39}$$

As the ratio of the NEEC and RR angular differential cross sections is rather small, the experimental observation of the NEEC signature is challenging. Nevertheless, knowing the angular pattern of NEEC is important as it provides a means of suppressing the RR background. Storage ring experiments focused on detecting the photons emitted in photorecombination have the best chances to observe the NEEC resonance at an angle of $\theta=142^\circ$ for the case of $E2$ transitions of the $^{174}_{70}$Yb nucleus.

IV. SUMMARY

In this work we consider the alignment of nuclear states formed in the process of nuclear excitation by electron capture. We calculate alignment parameters and geometric factors which determine the angular distribution of the subsequently emitted gamma photons. Such distribution functions are presented for a range of heavy elements with $E2$ nuclear deexcitation transitions. As the emission pattern of nuclear gamma photons is found to be substantially different from the emission characteristics of the background process of radiative recombination, our findings may help experimental attempts to discern NEEC from the competing process. For example, in the case of the $^{174}_{70}$Yb nucleus with an $E2$ transition, the best chance to observe the NEEC resonance is at an angle of $\theta=142^\circ$. This emphasizes the importance of measuring photon angle-resolved cross sections. Furthermore, the knowledge of the maxima and minima of the angular distribution of gamma radiation following NEEC is of general interest for any measurement aiming to observe NEEC.

ACKNOWLEDGMENTS

A.P. and Z.H. appreciate valuable discussions with Professor Werner Scheid. A.P. and U.D.J. acknowledge support from the Deutsche Forschungsgemeinschaft (DFG).

[1] V. Goldanskii and V. A. Namiot, Phys. Lett. **62B**, 393 (1976).
[2] K. Otozai, R. Arakawa, and T. Saito, Nucl. Phys. A **297**, 97 (1978).
[3] T. Saito, A. Shinohara, and K. Otozai, Phys. Lett. **92B**, 293 (1980).
[4] S. Kishimoto, Y. Yoda, M. Seto, Y. Kobayashi, S. Kitao, R. Haruki, T. Kawauchi, K. Fukutani, and T. Okano, Phys. Rev. Lett. **85**, 1831 (2000).
[5] T. Carreyre, M. Harston, M. Aiche, F. Bourgine, J. Chemin, G. Claverie, J. Goudour, J. Scheurer, F. Attallah, G. Bogaert *et al.*, Phys. Rev. C **62**, 024311 (2000).
[6] A. Pálffy, W. Scheid, and Z. Harman, Phys. Rev. A **73**, 012715 (2006).
[7] A. Pálffy, Z. Harman, and W. Scheid, Phys. Rev. A **75**, 012709 (2007).
[8] M. H. Chen and J. H. Scofield, Phys. Rev. A **52**, 2057 (1995).
[9] M. Gail, N. Grün, and W. Scheid, J. Phys. B **31**, 4645 (1998).
[10] S. Zakowicz, W. Scheid, and N. Grün, J. Phys. B **37**, 131 (2004).
[11] S. Zakowicz, Z. Harman, N. Grün, and W. Scheid, Phys. Rev. A **68**, 042711 (2003).
[12] T. Kandler, P. H. Mokler, T. Stöhlker, H. Geissel, H. Irnich, C. Kozhuharov, A. Kriessbach, M. Kucharski, G. Münzenberg, F. Nickel *et al.*, Phys. Lett. A **204**, 274 (1995).
[13] X. Ma, P. H. Mokler, F. Bosch, A. Gumberidze, C. Kozhuharov, D. Liesen, D. Sierpowski, Z. Stachura, T. Stöhlker, and A. Warczak, Phys. Rev. A **68**, 042712 (2003).
[14] G. Breit, R. Gluckstern, and J. Russell, Phys. Rev. **103**, 727 (1956).
[15] U. Fano and G. Racah, *Irreducible Tensorial Sets* (Academic Press, New York, 1959).
[16] J. Eichler and W. Meyerhof, *Relativistic Atomic Collisions* (Academic Press, San Diego, 1995).
[17] K. G. Dyall, I. P. Grant, C. T. Johnson, F. A. Parpia, and E. P. Plummer, Comput. Phys. Commun. **55**, 425 (1989).
[18] W. Greiner and J. Maruhn, *Nuclear Models* (Springer-Verlag, Berlin, 1996).
[19] P. Ring and P. Schuck, *The Nuclear Many-Body Problem* (Springer-Verlag, New York, 1980).
[20] A. R. Edmonds, *Angular Momentum in Quantum Mechanics* (Princeton University Press, Princeton, 1996).
[21] A. T. Ferguson, *Angular Correlation Method in Gamma-ray Spectroscopy* (North-Holland, Amsterdam, 1965).
[22] K. Siegbahn, *Alpha-, Beta-, and Gamma-Ray Spectroscopy* (North-Holland, New York, 1965).
[23] H. J. Rose and D. M. Brink, Rev. Mod. Phys. **39**, 306 (1967).
[24] V. V. Balashov *et al.*, *Theoretical Practicum in Nuclear and Atomic Physics* (Energoatomizdat, Moscow, 1984) (in Russian).
[25] A. Surzhykov, U. D. Jentschura, T. Stöhlker, and S. Fritzsche, Phys. Rev. A **73**, 032716 (2006).
[26] S. Raman, C. Nestor, and P. Tikkanen, At. Data Nucl. Data Tables **78**, 1 (2001).
[27] A. Surzhykov, S. Fritzsche, and P. Koval, Comput. Phys. Commun. **165**, 139 (2005).
[28] F. A. Parpia, C. Froese-Fischer, and I. P. Grant, Comput. Phys. Commun. **94**, 249 (1996).
[29] W. R. Johnson and G. Soff, At. Data Nucl. Data Tables **33**, 405 (1985).
[30] S. Fritzsche, A. Surzhykov, and T. Stöhlker, Phys. Rev. A **72**, 012704 (2005).
[31] S. Fritzsche, P. Indelicato, and T. Stöhlker, J. Phys. B **38**, S707 (2005).